EUROPEAN FUSION DEVELOPMENT AGREEMENT

EFDA–JET–PR(01)129

V. Pericoli Ridolfini, A. Ekedahl, S.K. Erents, J. Mailloux, S. Podda,
Y. Sarazin, A.A. Tuccillo and JET EFDA contributors

Study and Optimization of Lower Hybrid Waves Coupling in Advanced Scenario Plasmas in JET

Study and Optimization of Lower Hybrid Waves Coupling in Advanced Scenario Plasmas in JET

V. Pericoli Ridolfini[1], A. Ekedahl[2], S.K. Erents[3], J. Mailloux[3], S. Podda[1], Y. Sarazin[2], A.A. Tuccillo[1] and JET EFDA contributors

[1]Associazione Euratom ENEA sulla Fusione, Frascati, Roma, Italy
[2]Association Euratom-CEA, Cadarache, France
[3]Euratom/UKAEA Fusion Association, Culham, Abingdon, UK
** See the appendix of JET EFDA contributors (prpared by J. Paméla and E.R Solano), "Overview of JET Results",*
Fusion Energy 2002 (Proc. 19th Int. Conf. Lyon, 2002), IAEA, Vienna (2002).

Preprint of Paper to be submitted for publication in
Nuclear Fusion

ABSTRACT

A systematic study of the coupling of the Lower Hybrid (LH) power to JET plasmas has allowed us to overcome the problems of active current drive in the H-mode and ITB plasmas. As a result, LH power up to 4MW has been injected for longer than 8s in an ITB plasma. The LH coupling has been improved by fitting thepoloidal shapes of the plasma to that of the launcher, up to the degree allowed by the septum in the divertor, and by injecting deuterated methane (CD_4) from a pipe close to the LH antenna. Average values of the reflection coefficient as low as 4%, as in the previous L-mode operation are obtained. The reduced shape mismatch has strongly increased the poloidal uniformity of the plasma in front of the LH launcher and has permitted a balanced supply of the 3 grills. The major breakthrough, however, has been to puff CD_4, which increases the density in front of the LH launcher at least by 1.5 times locally, raising it above the cut-off value. This technique does not affects the plasma performances nor contaminates the main plasma up to the maximum flow rate so far used, $F_{CD4}>10^{22}$ el./s. Now it is routinely applied in JET and has allowed us to modify the plasma current radial profile evolution during the ITB, producing very encouraging results. Even though CD_4 is not suitable for ITER for the large tritium retention, the possibility to control locally and safely the scrape off plasma density has been demonstrated.

1. INTRODUCTION

The discovery of the internal transport barrier (ITB) regimes highlighted the potentiality of the lower hybrid (LH) waves as a tool to build and sustain the most advantageous radial shapes of the plasma current j(r), namely those with flat or even reversed safety factor profiles q(r). Initially, the LH power in JET was limited to the very early pre-ITB phase of the discharge, when j(r) is still evolving and the plasma is in a L-mode. In these conditions the power needed to trigger an ITB was strongly reduced, as a result of both LH heating and current drive (CD) [1]. As a natural forward step, the possibility of extending the LH pulse also during the ITB main phase was then considered and was the motivation for the present work. The ambition was to reach a true steady ITB by continuously controlling j(r), whose evolution can otherwise affect the ITB behavior even to the point to cause its termination.

ITB plasmas in JET with the Mark II Gas Box divertor usually exhibit an H-mode edge [2], and the coupling of waves in H-mode plasmas has been a serious problem in pre–EFDA JET. High reflection coefficients ($R_c \geq$ 20-30%) caused the 7MW of the LH power (P_{LH}) available for electron heating and current drive to be inefficiently used during the main heating phase of the pulse [2]. The poor coupling is due to the particular features of the H-mode scrape off layer (SOL) plasma. The typical SOL density scale length, λ_n, can be shorter than 1cm in high power discharges, while the antenna is set at 4-5cm behind the separatrix for safety reasons. This can bring the density in front of the LH launcher below the cut-off value ($n_{co} = 1.7 \cdot 10^{17}$ m^{-3} for the LH frequency $f_{LH} = 3.7$ GHz) [3] and therefore cause a total reflection. The trivial reduction of the distance plasma-LH antenna was not allowed because of a large influx of impurities, dangerous for the antenna itself

and for the plasma performance. Inaddition, the edge localized modes (ELMs), normally occurring in the H-mode caused frequent trips of the LH system, because of large reflected power imbalance, with a considerable reduction of the average coupled power [3]. With the start of EFDA JET a systematic study was begun on the methods to overcome the LH coupling problem without degrading the plasma performances and within the antenna safety limits. The following targets were fixed:

1) To work at the minimum plasma-launcher distance by installing a real-time control of the LH launcher position, under the safety limits imposed on the radiated power in front of the launcher and on the Fe influx;
2) To reduce significantly the number of trips by relaxing the protection system constraints on the allowed VSWR, by averaging the reflected power over a longer duration (100μs);
3) To improve the plasma homogeneity along the poloidal profile of the LH antenna by fitting at best the poloidal plasma shape to the antenna shape;
4) To control actively (increase) the SOL density in front of the LH launcher by injecting suitable gases from nearby pipes.

The first technique is in progress at present, whereas the second one has reduced the number of VSWR trips from 47% of the total to almost nothing. The remaining trips are produced by the protections against largely imbalanced reflections from the upper and lower part of the single LH multijunctions (MJ) that compose the LH grill (see Fig.1). In this paper we report the successful results obtained with the two latter methods. In Sec II we describe the organization of the experiment and the main experimental findings. In Sec. III we discuss the results and briefly survey the beneficial effects of LH current drive (LHCD) on the main ITB phase. In Sec. IV conclusions are drawn.

2. ORGANIZATION AND DEVELOPMENT OF THE EXPERIMENT

A picture of the JET LH launcher and of the nearby protection limiter, as seen from inside the vessel is shown in Fig.1(a). Its poloidal shape is compared in Fig.1(b) with that of the limiter, of a standard old ITB and of a typical discharge with optimized shape. The sketch of the cross section of one grill perpendicularly to the propagation of the waves is given in Fig.1(c). The antenna is formed by 3 superimposed equal grills, each made of 8 multijunctions arranged horizontally. One multijunction is a 4×4 waveguides matrix with 90^{o} constant phase step along the toroidal angle φ. The power is split poloidally inside the multijunction via a hybrid junction, in which the fourth port is connected to a vacuum load. The final matrix is 12 rows × 32 columns, and measures 89cm in height and 35.2cm in length [4]. More details on the LH system can be found in Refs. [5, 6] and references therein. For safety reasons in high power shots the launcher must be always in the shadow of the protection poloidal limiter, i.e. quite far from the LCMS (last closed magnetic surface). Consequently, the rapidly vanishing SOL density hinders a good coupling of the LH waves in plasma with an H-mode edge. As a further complication, for most ITB or H-mode configurations the density along the poloidal angle q is non-uniform. Indeed, a profile mismatch still persists between the actual LCMS and the antenna, despite the latter was poloidally shaped in the past to account for JET divertor operations. The variation

of the gap along q between the launcher and the LCMS is non negligible, since it can be even larger than the characteristic e-folding decay length of the SOL density λ_n ($\lambda_n \approx 1$cm). In addition, the length of the magnetic line (or connection length L_c) undergoes large and sharp jumps along θ. This in turn can affect the SOL parameters, as experimentally well documented in the FTU tokamak [7]. Indeed, ln increases with the connection length L_c: $\lambda_n \approx (D_\perp L_c/c_s)^{1/2}$, where $D_\perp$ is the transverse diffusion coefficient and cs is the sound speed. The Lc variation along q is due to the toroidal non-uniformity of the vacuum vessel walls, which is in practice unavoidable.

Figure 2 shows the magnitude of these two asymmetries effect on the poloidal pattern of the reflection coefficient R_c, for typical H-mode plasma. The abscissa z spans from bottom to top of the LH launcher. In frame a) L_c's are plotted, calculated along the actual profile of the LH antenna, and 8mm more inside in the vessel (3mm inside the limiter). In frame b) the gap LCMS-LH antenna is plotted. The bottom grill shows shorter connection lengths and a larger gap. Both these facts imply a lower density at the grill mouth and concur to form the reflection pattern shown in frame c) an R_c value as high as 15%, as it is found on the lower row of the bottom grill, means a plasma density close to the cut-off value. Attempts to discriminate the effects of $Lc_c(z)$ from those of the gap were made by varying the extent of the private SOL region (that in between the limiter and the antenna) while keeping constant the total LCMS-antenna gap. No significant change of Rc was however observed even for the bottom grill, which should have been the most sensitive to density variations because of the poorest coupling. Indeed, this action affects only slightly the pattern of L_c in front of the grill in question, as the closeness of the two traces in Fig. 2 a) suggest. By contrast, equalizing the gap along θ implies to reshape the LCMS, which in turn modifies the field line trajectories and causes L_c's also to be more uniform.

A standard procedure has been then developed to better match the shape of the separatrix to that of the antenna. It essentially consists of two tools. On JET usual plasmas, the magnetic axis is about 0.3m above the equatorial plane, while the LH launcher is symmetric astride it (±0.44m). Increasing the current (opposite to the plasma current Ip) in the divertor poloidal coil located in the low B_T side (B_T is the toroidal magnetic field) leads to a movement of the X-point toward the inner target (high field side). Maintaining the LCMS-limiter distance constant, the outer lower part of the separatrix then bends up, and gets closer to the lower rows of the LH launcher. A drawback is that this may also lead to a worse matching of the upper rows. In this case, decreasing the top outer gap may counterbalance this effect. This latter technique produces more elongated plasmas. The shape optimization can be quantified by measuring the dispersion of the LCMS-antenna gap, G, along the poloidal angle. The smaller is G the better is the coupling. Figure 3 compares the maximum dispersion along q of the LCMS–LH antenna gap, for the well matched OS (optimized shear) plasma Pulse No: 51552 with a standard OS configuration of the previous campaign (Pulse No: 49651) and with a non optimized high bp ITB plasmas (Pulse No: 51930). The former exhibits an improvement by a factor of about 3 with regard to the second one, and by a factor of about 7 with regard to the third one.

As a result, the distance between the LCMS and the limiter can be maintained as small as about

4cm with the LH grill only 6mm in the limiter shadow both in the preheat and in the main heating phase of ITB plasmas, with a total power in excess of 20MW, whereas at lower power (≈13MW) even 2cm and 5mm respectively can be sustained.

In JET the ion cyclotron resonance heating, ICRH, is expected to possibly affect the LH operation, differently from the neutral beam injection, NBI. The fast ions with large Larmor radii generated by the ICRH waves can sputter from the LH antenna large quantities of metals, which in turn pollute the plasma. The high ICRH electric fields in the proximity of the antenna may disturb the edge plasma as well. The compatibility between the LH and ICRH systems has been investigated in JET under the following conditions: H-minority heating scheme, with the H-resonance inside about 1/3 of the minor radius, ICRH power $P_{ICRH} \leq 8$MW (Pulse No: 51136). Minority H concentration (n_H) less than 4% can make unsafe the LH operation. Good LH coupling requires that the power generated by the closest ICRH antenna (antenna B) does not exceed 1.8MW. No limitation is found on other antennae (A, C, D). The reason lies in the fact that only the antenna B is magnetically well connected to the LH launcher, as shown in Fig.4. Here three field lines originating at the center of the three LH grills are plotted in a θ–φ plane, and the four ICRH antennas are sketched as rectangles. It is also sketched the location of the reciprocating Langmuir probes (RLP, A and B), used for the SOL measurements, and of the two gas valves utilized for the gas inlet (GIM6 for CD_4 and GIM8 for D_2). At the vessel bottom ($\theta \approx -90^o$) all the lines are stopped by the divertor plates, whereas their prosecution at $\varphi < 0^o$ is reported at $\varphi < 360^o$.

Quantitative comparison between the antenna B and the others is made in Fig.5 where the average reflection coefficient R_c for each of the three LH grills is plotted versus the local edge density. This latter is evaluated assuming: $n_{e,LH} \propto H_\alpha \bullet e\text{-}dx\ l\ n\ x\ (\ )d\grave{o}0 = H\ a \bullet ek\ dx\ Lc\ x\ (\ )\ \grave{o}0$ with H_α =brilliance of the D_α line, d=LCMS-LH grill distance. The integration is performed along the perpendicular to LCMS towards each grill. The proportionality factor k is fixed by the ratio $n_{e,LH}/n_{e,LCMS}$, which is in turn estimated from RLP measurements in a similar H-mode discharge. The ne values are then normalized to the maximum density. In this case, with the LCMS shape almost optimized, the highest density is found in front of the lowest grill, which consequently shows the best coupling. From Fig.5 it appears the usual feature that the poorer coupled grill is the most sensitive to variations of the edge conditions, either if the coupling improves or if it degrades (see also later).

Influence of the ICRH power on LH coupling is observed also in Tore Supra, see Ref. [8] and references therein. Here, with the aid of Langmuir probes on the LH launchers [8], it has been recently found that the density decreases on the probes connected to an ICRH antenna, and then the LH coupling deteriorates, while the density on the probe not connected stays constant, in agreement with the present results.

The active control of the density in JET in front of the LH grill was already attempted in the past by puffing D_2 gas from a nearby pipe [9, 10]. The success of the experiment however was counteracted by the large amount of gas flow requested, which caused variation of the main plasma parameters and degradation of the ITB performance [3]. On the other hand, during the study of

transport of hydrocarbides in tokamaks, the injection of methane (CD_4) in L-mode plasmas was found to lead to an increase in the SOL electron density larger than D_2. Conversely, both the electron temperature and density at the separatrix remained unchanged, as well as all the main properties of the core plasma [11]. This suggests that most of CD_4 is ionized in the SOL and subsequently removed by parallel transport to the divertor.

This consequence pushed strongly to test CD_4 also in the H-mode and/or ITB plasmas in order to improve LH coupling. The outcome of the relevant experiments is reported in the following figures. Figure 6 compares the Rc values along the LH antenna height for a shot with CD_4 at a flow rate $\Phi_{CD4}=10^{22}$ el./s (Pulse No:51121), and for one without CD_4 (Pulse No:51120). The improvement of Rc due to CD4 is larger for poorer coupling conditions.

In these shots the up-down asymmetry in the LCMS-antenna gap was not fully corrected to investigate better the effect of CD_4 injection. The uppermost grill shows a higher R_c value, because the whole reflection pattern is modified by protections on several multijunctions. On these two shots the experimental reflection pattern is compared with the predictions of the LH multijunction coupling code SWAN. The code needed to be adapted [12] to account for the actual dimensions of the front end of the LH antenna. Indeed, when JET started divertor operations, the poloidal shape of the grill was modified to match that of the LCMS. For each row of the antenna, the new calculations yield the power reflection coefficients and phases, as seen from the hybrid junctions inside the multijunctions towards the 4-waveguide sections. These values are then compared with the experimental ones as done in Fig.7(a) and 7(b). The middle part of the launcher (rows 3 & 4) has been chosen, since all multijunctions in these rows were fed with equal power and no interrupts occurred there. The agreement with experiment is satisfactory.

The new version of the code can account for the low R_c on the extreme waveguides of row 4, while the old version could not. Also the difference in the average values of Rc between rows 3 and 4 is reproduced with the same edge density. The estimated increase in the electron density in front of the launcher, following the injection of CD_4, is from 2 to $3\cdot10^{17}$ m^{-3}. A vacuum gap in front of the waveguides of d_{vac} = 1mm is assumed in both cases. Although the absolute density increase may not seem large, the effect on the coupling is significant at these low levels of electron density, i.e. close to the cut-off density ($n_{co}=1.7\cdot10^{17}$ m^{-3}). The improvement in R_c as measured at the back of the multijunctions corresponds to a much larger improvement in the power reflection coefficient at the grill mouth and hence to a considerably higher power handling capability. For instance a decrease of Rc from 10% to 4% produces at the grill mouth a drop from 32% to 20% of the reflection, and by 16% of the maximum voltage. If wanting to keep this latter at the same level, the obtained reduction in reflection coefficient would allow increasing the launched power by 35% [13].

The effects of the CD4 injection on the LH coupling and on the main plasma parameters in a H-mode discharge are reported in the Figs. 8, 9, 10 and 11, as the time traces of the relevant quantities. The typical parameter of the H-mode are: magnetic toroidal field, $B_T=2.6$T, $I_p=2.5$ MA, line averaged density $n_e\approx2\cdot10^{19}$ m^{-3}.

Figure 8 shows the time traces of the quantities more relevant for the edge plasma behavior. In frame a) the three powers, NBI, ICRH and LHCD are plotted. In b) the total LH reflection coefficient is shown: the enhancement in the LH coupling, following CD_4 puff, is emphasized by the drop in Rc from about 10% to 4% and by the lower noise due to the rarefaction of the LH system trips. The delay of the coupling improvement on the CD_4 puff, shown in frame e), is due to the neutral gas diffusion time from the CD_4 valve, called GIM6, to the LCMS. The temporal evolution of the CIII UV line ($\lambda = 97.70$nm), frame c), indicates that the C influx is totally negligible. No C accumulation effects in the JET walls has been observed up to now, even after several days of operations with prolonged (several seconds) CD_4 injection. The evolution of the FeXXIII UV line ($\lambda = 13.29$nm, frame d), testifies that there is no interaction of the LH antenna with either the plasma or the ICRH fast ions, despite the low LCMS-limiter gap and the thin private SOL, respectively 20 and 5mm, frame f).

Figure 9 exemplifies that the CD4 injection does not affect noticeably the main features of ITB plasma, even for large CD_4 flux ($\Phi_{CD_4} = 10^{22}$ el./s): no change occurs in either the peak ion temperature and in its radial profile, or in the energy confinement. On the contrary, the ELMs activity is modified. The general trend is an increase of the ELM frequency and a decrease of their amplitude [14]. In the case of Fig.9 they are completely suppressed [15].

The behavior of the ELMs as a function of the CD_4 flow rate is presented in Fig.10 (a) and (b), where it is compared with the argon injection, for a series of shots with the total additional power $P_{add} > 14$MW. Similarly to Ar, CD_4 appears to reduce the ELM frequency and (to a less extent) their magnitude. The ELM frequency ranges from ≈250 Hz up to ≈450Hz, while the ELM magnitude (defined here as the maxima in the D_α emission) is almost divided by a factor of two, when Φ_{CD_4} increases from 0 to $8 \cdot 10^{21}$el./s, and it is turned to 0 at $\Phi_{CD_4} \bullet 10^{22}$ el./s. The physical mechanism leading to such a modification of the ELM dynamics is still unclear. Possible explanations include larger radiative losses, increase in the edge resistivity, and modification of edge plasma current, which is thought to play a prominent role in type-III to type-I ELM transition [2, 16]. In Fig. 11 the change in the bolometric losses, though small, is documented as a slight peripheral peaking in the radial profile. The constancy of the effective ion charge Z_{eff} under CD_4 flow is also presented.

We point out, however, that this picture could substantially change once the gas box divertor is modified by removing the central septum. The more open configuration, could well affect the recycling in the divertor and the ELMs dynamics.

The effects of CD_4 on the main plasma have been compared with those produced by injecting D_2 at a rate high enough to improve similarly the LH coupling. As already observed [10], this affects negatively the plasma performances in JET, but the method had not yet been tested in a H-mode edge and with an optimized LCMS shape. We chose to puff the extra D_2 from GIM8 valve, which is located at the torus top at $\varphi = -45°$, since it was not possible to switch GIM6 quickly from CD_4 to D_2. GIM8 is not fully connected magnetically to the LH launcher, particularly to the lower grill, see Fig.4, but its shadow is not too far away. This latter distance is easily covered by the

diffusion of the neutrals during their travel from GIM8 to the LCMS, which expands the effective extent of the GIM8 flux bundle. Consequently, the LH antenna should see an increase of nedge, even if this latter were bounded to the flux cEndle where ionization takes place, as it happens with CD_4 [17].

Two ELMy H-mode shots are compared in Fig.12, Pulse No: 51008 and Pulse No: 51011. They both exhibit benign ELMs, and the power crossing the separatrix exceeds the standard L to H-mode power threshold [18] by a factor of order of 3. The LH coupling improves with D_2 as much as with CD_4 for similar electron injection rates, and it is less pronounced for the grill magnetically far from the gas source. D_2 and CD_4 apparently then produce a similar increase of the SOL density, but the effects on the main plasma are different: D_2 does penetrate into the main plasma, and raises the density, while CD_4 does not. In that respect, puffing D_2 does not seem appealing for improving LH coupling in H-mode, as further stressed in the following section.

3. DISCUSSION

The choice of CD_4 to control the edge density was not only heuristic, but it was suggested also by its known low transport across the SOL, discussed in Ref. [19]. This latter is due to the fact that all the fragments of the dissociation chain of the CD_4 molecule are quickly ionized within the SOL and then they drift only along the magnetic field lines towards the divertor. Compared to hydrogen, the ionization potentials E_i are quite low and the ionization rates $<\sigma v>i$ high (σ is the cross section and v is the velocity of the background electrons, on whose distribution averaging is made). E_i,CDn ranges between 12.5eV for CD_4 and 9.8eV for the CD_3 radical [20], while the total $<\sigma v>_i$ at $T_e = 20$ eV is close to 10^{-13} $m^3 \cdot s^{-1}$, against 13.6eV and $1.5 \cdot 10^{-14}$ $m^3 \cdot s^{-1}$ for H, respectively. In addition, the cross-field transport due to charge exchange processes, which is efficient for H, remains low for CD_4 because the molecules do not survive long enough to equilibrate thermally with the background ions [19]. Therefore, the effective perpendicular neutral velocity is substantially the thermal one of the puffed particles, whose temperature is about 0.03eV. This low value is the main difference with the C neutrals sputtered from the walls.

The increase of the SOL density due to CD_4 puffing, without significant effects inside the LCMS, is well documented in JET with the gas box divertor, in Ref [17]. The increase appears to be bounded essentially to the flux tube connected with the gas source, i.e. with the region where most of the ionization occurs. However, the actual reason for the ne rise it is still unclear according to numerical modeling. The model confirms that most of the CD_4 ionization does occur within the SOL, but predicts that this higher ionization rate would be balanced by a faster plasma flow towards the divertor plates. Change in the perpendicular transport is proposed to account for the experimental density increment.

Independently of the physical mechanism at work, the perturbed region is the flux tube connected with the ionization source. However the reciprocating probes measurements of the present work suggest that the methane molecules are ionized in different sites for the L and H mode in JET. This

is inferred from the comparison of the SOL density profiles with or without CD_4 injection, plotted in Figs.13(a) and (b), respectively for the L and H mode.

The data are taken from probe B, which is located at the top of the octant 5 ($\varphi_B = 187^o$), while the probe A ($\varphi_A = 7^o$) checks that no changes are occurring in the SOL outside the CD_4 temporal window. Methane gas is injected into the discharge from GIM6 pipe, as said before. When CD_4 is puffed, the SOL density in L-mode is more than doubled at the radial position of the LH antenna and remains unaltered at LCMS, whereas in H-mode it is unchanged all along the SOL width, within the experimental errors. On the other hand, nedge does increase also in the H mode in front of the LH antenna, otherwise the large improvement of the LH coupling would hardly be explained: an increment by a factor 1.5 at least is needed, as shown previously in Fig.8. Consequently, the ionization source appears to be magnetically connected to the probe B in L mode, and not connected in H mode. Since the magnetic lines trajectories in the SOL are almost indistinguishable for the presented discharges, the regions with strong CD_4 ionization must be differently located.

The fact that in L mode the probe B records a ne increase but it is not magnetically connected to the projection of GIM6 onto LCMS (see Fig.4) must not surprise. Indeed, the ionization region cannot be strictly identified with the geometrical shape of the gas source, as obtained from a straight projection onto LCMS. Its contours are enlarged by the diffusion of the neutrals before ionization. A divergence of the neutral flux in the vertical direction of only 26^o, well below that of a gas nozzle, would be sufficient to wet a portion of the SOL, which does connect magnetically to the probe B.

Ionization of CD_4 in H mode within a zone of the SOL, connected to the LH antenna but not to the probe B, can occur by two ways. The first one is ionization ahead the gas pipe by background SOL electrons. This should take place mostly in the SOL sufficiently far from LCMS, so that the magnetic lines are stopped by the protection limiter (between the launcher and the ICRH antenna "B" see Fig. 1(a)) and cannot reach the probe, see Fig.4. The second way is direct ionization by the LH electric fields in front of the grill. In this case, the ion source region would be precisely delimited by the LH grill profile and would be no more connected to the probe B, as shown in Fig.4. These two mechanisms can operate also together, and are made possible by the large ionization rate of CD_4 compared to H.

Ionization rate of CD_4 by the background electrons in the far SOL can indeed increase substantially in H mode with respect to L mode, because of the higher electron temperature. As shown in Fig.14, the H-mode SOL temperatures are clearly higher by about 15–20eV over all the radial profile, despite the lower quality of the data. Such a ΔT_e has a very large effect on $\langle\sigma v\rangle_{i,CD_4}$, which is a very rapidly increasing function of T_e, in the range $5 \leq T_e \leq 10$eV, and at 20eV is very close to its top value [19]. We must however not forget that both density and temperature of the SOL in front of the LH grill and of the GIM6 gas pipe could be lower than those inferred from Figs. 13 and 14 by two causes: 1) the magnetic lines are shorter than for the probe, because they are stopped on one side by the limiter and on the other side by the bottom divertor, see Fig.4; 2) the proximity of the protection limiter further depresses both ne and Te.

On the other hand, the LH electric field (in JET: $_{ELH}$[V/m]≈4.62·10^4 ·P_{LH}[MW]$^{1/2}$), is strong enough to increase significantly the electron impact ionization rate of the CD_4 molecule in the SOL. Responsible of that is not however the sloshing energy acquired in the oscillatory field, which would be too low for the purpose (W_{sl}[eV]≈0.34·P_{LH}[MW]), but it is the instantaneous energy gained from the work done in half period by E_{LH} during the actual displacement of the electrons. In this picture only half of the electrons will be accelerated by E_{LH}, whereas the other half (that with the 'wrong' sign of the velocity) will be retarded. The average energy gained from the field is nil of course, but the 'right' half of the electrons could become enough energetic to enhance ionization. Details on these estimates are given in the appendix, where it is also shown how the experimental neutral flow rate, required to improve the LH coupling, is consistent with this description.

In this picture of quite localized density increase, also the SOL modifications directly induced by the LH power should be evaluated. Significant changes in Te are not expected because the power lost by the LH waves in the whole SOL is negligible: less than 0.35% of the total. This has been roughly estimated from the sloshing energy that thermal electrons can extract from the LH resonance cones per unit of time (the process considered above with average zero electron energy does not contribute of course). Increase of T_e was not observed also in other LH experiments on tokamaks, even in the flux tubes directly connected with the antenna [21]. By contrast, decrease of the SOL density was either directly measured [21] or inferred from the non-linear behavior of the LH reflection coefficient [22], and was attributed to ponderomotive forces due to the LH power. For JET however, the sloshing energy in the SOL is to small with respect to the electron thermal energy to produce important effects: calculations performed in the same way as in Ref [21] give less than 10% reduction of the density.

Experimentally it has not been possible to discriminate between the two effects at JET. No CCD camera was available to look at the region surrounding the grill mouth for possible increased ionization, nor there was any RLP directly connected to the LH antenna without the interposition of the limiter, to seek for peculiar SOL radial profiles.

It must be pointed out that the SOL characteristics could change for a different configuration of the divertor, so that the general response to CD_4 injection, also in terms of the impurity retention, can be quite different as well, if a more open divertor will be adopted.

3.1 LHCD EFFECTS ON ITB PLASMAS

In the same experimental campaign devoted to study the LH coupling during an ITB in JET, described in the present paper, we demonstrated also for the first time that the favorable transport properties of an ITB can be preserved for a longer time by applying LHCD during the main heating phase [14, 15]. A clear example of that is shown in Fig. 15, where we compare two identical discharges except for the application of LHCD, Pulse No: 51490 with LHCD and Pulse No: 51491 without. In the discharge with LHCD the onset of the ITB is more prompt and lasts longer than 2.5s, until the end of the main heating phase (NBI+ICRH). The ITB can also recover from several partial collapses.

Conversely, in the discharge without LHCD the ITB lasts less than 1 s and it is terminated at the first collapse.

On these bases a lot of work has then been started and very good results have been obtained, which strongly widen the way towards a steady ITB. In Refs. [23] and [24] it is shown how the LHCD applied during an ITB can extend the ITB lifetime up to about 10s, which is the timescale of the current diffusion. The most important effect of the LHCD is to slow down substantially the time evolution of the safety factor profile during the ITB. Since a weak negative or flat shear of q(r) is a key ingredient for onset and development of an ITB the importance of preserving it is straightforward.

CONCLUSIONS

The experiments conducted at JET to improve the LH coupling during both the H-mode and ITB plasma have permitted an exploitation of the LHCD potentialities in these regimes. Up to 4MW of LH power could be coupled to ITB plasmas for longer than 7-8s and at high additional power ($P_{NBI + ICRH} + P_{LH} > 20MW$), by simultaneously optimizing the plasma shape and continuously puffing CD_4 from a pipe close to the launcher. In a typical H-mode the reflection coefficient has been dropped from $R_c > 20\%$ in the pre EFDA JET to $R_c \approx 4\%$, still maintaining the LH antenna far enough from the separatrix for a safe operation. This is a very large step forward for a multijunction grill, and the specific contribution of CD_4 is to reduce Rc from about 10% to 4%, which is a remarkable progress too. A density increase in front of the grill mouth larger than 1.5 times can account for the observed R_c improvement. The involved ion source within the SOL is located differently in H and L mode. In H mode it appears more delimited and this is compatible with ionization both from the SOL background electrons or directly from the LH power. No counter indication has been so far raised against puffing CD_4. Evidence of negligible recycling on the JET first wall comes from the fact that the coupling improvement lasts just as long as the CD_4 time window. Neither accumulation nor influx of impurities have ever been detected, no deterioration of ITBs has been observed. The possibility to further increase P_{LH} by this method is then open, even though at $P_{LH} \geq 5MW$ limitations on the maximum allowed gas flow rate cannot be excluded, as in the old D2 assisted LH coupling experiments.

CD_4 injection cumulates the advantages of both D_2 and Ar puffs without exhibiting their drawbacks. Similarly to D_2, CD_4 improves the LH coupling, but it does not affect the central density or the H-mode quality, and similarly to Ar, it modifies the type III ELMs behavior, but does not perturb T_i and v_j (rotation velocity) measurements.

We must also remark that the dynamics of CD_4 could be modified if the divertor is changed from the present gas box to a more open configuration.

By contrast, the use of such a technique is not of immediate use for ITER because of the large tritium retention in carbon. Nevertheless, the path towards an ITER-like configuration (LH antenna flush with the walls) has been tracked.

At present, the use of other interesting gases, which could be of more direct interest for ITER, is

still to be investigated. These could be SiD4, with chemical properties similar to CD_4, or disilane Si_2H_6, with even lower ionization potential also for the dissociation chain (≈7.8eV), or gases with lighter elements as diborane B_2H_6, whose E_i is = 11.38eV. To proceed along this route it is essential however to prove that the residual electron density in front of the LH waveguides for very far distance from LCMS is still capable of providing a sufficient seed to ionize the extra gas puffed.

APPENDIX

EVALUATION OF THE IONIZATION OF CD_4 DIRECTLY BY THE LH FIELDS IN JET

The LH electric field and the associated electron sloshing energy are given in JET by:

$$P_{LH}\,(V/m) \approx 4.62 \cdot 10^4 \cdot \sqrt{P_{LH}\,(MW)} \tag{1}$$

$$W_{sl}\,(eV) \approx 0.34 \cdot P_{LH}\,(MW) \tag{2}$$

Therefore, W_{sl} is ≤1eV for the usual LH power level: P_{LH}≤3 MW (≈1MW/grill), and it is too small to affect significantly the CD4 ionization rate, $\langle\sigma v\rangle_i,CD_4$. This latter is a very rapidly increasing function of T_e, in the range $5 \le T_e \le 10$eV, and at 20eV is very close to its top value [19]. Even by considering the instantaneous energy, to which ionization is actually sensitive, the gain would be only a factor 2, which is still too small. But the work done by E_{LH} on a single electron during its actual displacement in half the period of the wave can give it enough energy for ionization. Of course, only half of the e- distribution function will be accelerated by E_{LH}, whereas the other half (with the 'wrong' sign of the velocity) will be retarded so that the average energy gained from the field is nil.

In the following calculations we suppose that the electrons do not see the wave spatial structure of E_{LH}, which therefore is assumed constant and parallel to the magnetic field. Indeed, for T_e=10eV the displacement of a thermal electron during a LH half period, is only $\ell_{\parallel,th} = v_{\parallel,th}/2f_{LH} \approx 0.18$mm, against the LH parallel wavelength $\lambda_{\parallel,LH} = \lambda_0/N_\parallel \approx 45$mm ($v_\parallel$ is the electron parallel velocity, f_{LH} the LH frequency = 3.7GHz, λ_0 the vacuum wavelength=81 mm, $N_\parallel$ the parallel refractive index ≈1.8). The electron energy increment is therefore:

$$\Delta W = -eE_{LH} \int_0^{T_{LH}/2} \sin(\omega t + k_\parallel z_0) \cdot v_\parallel dt = -2eE_{LH} \cos(k_\parallel z_0)\, \frac{v_\parallel}{\omega} = -2eE_{LH} \cos(k_\parallel z_0) \frac{\ell_{\parallel,th}}{\pi} \tag{3}$$

Here e and m_e are the electron charge and mass respectively, $T_{LH} = 1/f_{LH}$ is the LH period, $\omega = 2\pi f_{LH}$, $k_\parallel = 2\pi/\lambda_\parallel$,LH is the LH parallel wave vector. For a thermal electron, averaging on the spatial phase $k_\parallel z_0$ (only on the positive cosine values, as said before, which gives a factor $2/\pi$) and using Eq. (1), one gets:

$$\Delta W_{th}\,(eV) = E_{LH} \frac{4}{\pi^2} \ell_{\parallel,th} \approx 3.37 \sqrt{P_{LH}\,(MW)} \tag{4}$$

Typically $P_{LH} \approx 3MW$ so that $\Delta W_{th} \approx 5.8eV$. This energy gain is not negligible when dealing with the ionization of molecules like CD_4 and with electron temperatures in the range of 10eV. Adding this energy increment to the sloshing motion the total gain is

$$\Delta W_{tot} = \Delta W_{th} + 2W_{sl} = 3.37 \sqrt{P_{LH}} + 0.68 \cdot P_{LH} \tag{5}$$

Which amounts to 7.9eV approximately. By comparing ΔW_{tot} with the minimum threshold of the ionization potentials of the CD_4 dissociation chain ($E_{i,min} = 9.8eV$), we see that the energy gain is enough to give the thermal electron the maximum reaction rate. Since only half electrons are involved, the total ionization rate will be close to half its top value. The other half electrons still contribute to ionization provided the unperturbed energy W_0 satisfies the relation $W_0+2W_{sl}-\Delta W>E_{i,min}$. By contrast, the value of $\langle\sigma v\rangle_i$ without the LH power is 10 times below the maximum [19], for the temperatures expected in front of the grill, see Fig.14.

The LH power lost in these processes is a negligible fraction of the total. It can be estimated from the loss rate of the electrons generated in front of the LH antenna. If $n_{e,LH}$ is their average density, h and $L_{||}$ are the height and length of the LH antenna, e_r is the radial depth of the ionization layer, $\tau_{||}$ is their dwell time, we get for the ionization power loss P_{ion}:

$$P_{ion} = \frac{n_{e,LH} L_{||} h e_r}{\tau_{||}} \cdot E_i = n_{e,LH} c_s h e_r E_i \tag{6}$$

For the sake of the plasma quasi-neutrality, the electron velocity $L_{||}/\tau_{||}$ is assumed equal to the CD_4 ion drift velocity, given by the sound speed c_s. As shown in Ref. [19] the thermalization of the CD_4 ions is largely incomplete, so that at good approximation

$T_{CD_4} = 0.1 \cdot T_e \approx 1eV$, $c_{s,CD_4} = 9.79 \cdot 10^3 \frac{T_{CD_4}(eV)}{\mu_{CD_4}} \frac{m}{s} \approx 2.45 \cdot 10^3 \frac{m}{s}$ ($\mu CD_4 = 16$ is the CD4 molecular weight). Fixing $e_r = 0.03m$, $h = 0.89m$, $n_{e,LH} = 2 \cdot 10^{17}\ m^{-3}$, one gets $P_{ion} = 21W$. Even considering that the atomic radiation can make the effective power loss even 5 times bigger, we still have negligible values.

The gas flow rate needed to increase the density in front of the LH grill is estimated assuming that there the particle balance is dominated by the ionization processes, rather than by diffusion across the SOL. In such a region, the charged particles balance imposes that at the stationary state the overall ion source is equal to the volume loss of neutrals, given by the divergence of the neutral flux, i.e. $\nabla\Phi_n \approx n_n v_n/\ell_n$, where n_n, v_n and ℓ_n are the neutral density, velocity and decay length. The ions are removed from this volume by streaming along the magnetic field lines, i.e. the drain term is: $-S_i = n_i/\tau_d$, where $\tau_d = L_{||}/c_s, CD_4$ is the dwell time in front of the LH grill, whose length along the magnetic line is $L_{||} \approx \sqrt{2}\ L_{\varphi,LH} \approx 0.5m$ ($L_{\varphi,LH} = 0.38m$, is the length in the toroidal direction). Assuming ne=ni, the balance between the ion source and loss can be written as:

$$\frac{n_n v_n}{\ell_n} = \frac{n_e v_n}{\tau_d} \Rightarrow n_n = n_e \frac{\tau_{mfp}}{\tau_d} = \frac{1}{\tau_d \langle\sigma v_e\rangle} \Rightarrow n_n = \frac{c_{s,CD_4}}{L_{||}\langle\sigma v_e\rangle} \tag{7}$$

The obtained expression for n_n is the well-known lower limit to the neutral density for a SOL where ionization dominates over cross-field diffusion [25]. In Eq. (7) we used the relation $v_n/\ell_n = 1/\tau_{mfp} = n_e\langle\sigma v_e\rangle_i$ (τ_{mfp} is the neutrals mean free path). The neutral density can be estimated from the neutral source strength G_n (particles/s) and the geometry of the system GIM6 pipe – LH antenna. Assuming for simplicity that the gas pipe is a line segment of height $l_p \approx 1$m, the particle flux onto the LH antenna, which is distant $r \approx 1$m is high $h_{LH} \approx 0.89\text{m} < l_p$, can be approximated as it were perpendicular to the pipe. This is acceptable until the linear extension of the source is of the order the distance considered, and it is larger than the wetted object. We obtain therefore:

$$\Phi_n \ \pi r h_{LH} = G_n \ \frac{h_{LH}}{l_p} \Rightarrow G_n = n_n \, v_n \pi r l_p \tag{8}$$

Substituting for n_n in Eq. (7) we obtain for the neutral source strength the lower limit:

$$G_n \geq \frac{\pi r l_p c_{sCD_4}^2}{L_{||}\langle\sigma v_e\rangle_i} \geq 4\cdot 10^{20} \text{ particles/s} = 4\cdot 10^{21} \text{ el.s} \tag{9}$$

G_n has been evaluated supposing that $T_{CD4} = 0.1\cdot T_e \approx 1$eV, as before. The term $\langle\sigma v_e\rangle_i$ in Eq. (9) should be representative of the global ionization rate, for which we assumed the CD4 top value $\langle\sigma v_e\rangle_i \approx 10^{-13}\ m^3\cdot s^{-1}$.

The lower limit to G_n given in Eq. (9) is just the one above which the improvement in the LH coupling is indeed observed, see Ref [14] and Fig. 12.

REFERENCES:

[1]. CHALLIS, C.D., BARANOV, Y.F., CONWAY G.D., GORMEZANO, C., GOWERS, C.W., et al., Plasma Phys. Controll. Fusion **43**, 861-879 (2001).

[2]. The JET team (presented by F.X. SÖLDNER) et al., Plasma Phys. Control. Fusion **39**, B353 (1997).

[3]. JOFFRIN, E., et al., JET report JET-R(99)09 (1999).

[4]. LITAUDON, X. and MOREAU, D., Nuclear Fusion **30**, 471 (1990).

[5]. Ph. Schild, J. A. Dobbing, A. Ekedahl, M. Goniche, C. Gormezano, M. Lennholm, F. Söldner, "Improvement of Power Handling and Operation of the LHCD System on JET", Proc. 17 th Symposium on Fusion Engineering, San Diego, California, USA, 1997. New York: IEEE **Vol. 1**, p. 421, (1998)

[6]. M. Lennholm, Y. Baranov, J. A. Dobbing, A. Ekedahl, P. Finburg, B. Fischer, C. Gormezano et al, "Operation of the 3.7 GHz LHCD System in JET", Proc. 16 th Symposium on Fusion Engineering, Urbana-Champaign, Illinois, USA, 1995. New York: IEEE, **Vol. 1**, p. 754, (1996).

[7]. LEIGHEB, M., PERICOLI RIDOLFINI, V., ZAGÓRSKI, R., J. Nucl. Mat., **241-243**, p. 914, (1997)

[8]. A. Ekedahl and L. Colas, "Density modification in front of radiating ICRH antennas and the effect of the coupling of Lower Hybrid Waves", xxxx 2002.

[9]. EKEDAHL, A., BARANOV, Y., DOBBING, J.A., FISCHER, B., GONICHE, M.. et al. Radio Frequency Power in Plasmas (Proceedings 12 th Topical Conference, Savannah, 1997), AIP Conf. Proceedings **403**, 169-172. (1997).

[10]. GONICHE, M., DOBBING, J.A., EKEDAHL, A., SCHILD, P., SÖLDNER, F.X., JET report JET-R(97)14 (1997) 'Long distance coupling of lower hybrid waves in JET using gas feed'.

[11]. STRACHAN, J.D., FUNDAMENSKI, W., CHARLET, M., ERENTS, S.K., GAFERT, J., et al. 'JET methane screening experiments', to be published in Nuclear Fusion

[12]. EKEDAHL, A., BIBET, P., LENNHOLM, M., LITAUDON, X., MAILLOUX, J., PERICOLI RIDOLFINI, V., SARAZIN, Y., TUCCILLO, A.A., et al., in Radiofrequency Power in Plasmas (Proc. 14 th Top. Conf., Oxnard, USA, 2001) AIP Conf. Proceedings 595, 249 – 252, (2001).

[13]. J A Dobbing, A Ekedahl, P Finburg, B Fischer, C Gormezano, M Lennholm, J Romero, P Schild, F X Söldner, "Power Handling in the JET Lower Hybrid Launcher", JET Report JET-R(97)06 (1997).

[14]. SARAZIN, Y., PERICOLI RIDOLFINI, V., BARANOV, Y., CHALLIS, C.D., EKEDAHL, A., Proc. 28 th European Conf. on Controlled Fusion and Plasma Physics, Funchal, Portugal, 18-22 June 2001, Europhysics Conference Abstracts **Vol. 25A**, p. 1661- 1664, (2001).

[15]. PERICOLI RIDOLFINI, V., PODDA, S., MAILLOUX, J., SARAZIN, Y., BARANOV, Y., et al., in Radiofrequency Power in Plasmas (Proc. 14 th Top. Conf., Oxnard, USA, 2001) AIP Conf. Proceedings 595, 245 - 248, (2001).

[16]. Y. Sarazin, M. Bécoulet et al., submitted to PPCF.

[17]. G. F. MATTHEWS, ERENTS, S.K., CORRIGAN, G., FUNDAMENSKI, W., GARCIA-CORTES, I., et al., 'The effect of CD4 puffing in the peripheral Scrape-off layer in JET', to be published in PPCF.

[18]. ITER confinement database and modeling expert group, (presented by T. Takizuka) "Threshold power and energy confinement for ITER", in Fusion Energy 1996, Proc. 16 th Int. Conf. Montreal, Canada, 1996) **V. 1** (Vienna, IAEA) p. 603, (1997).

[19]. W. D. LANGER, Nucl. Fus., **22**, 751-761, (1982).

[20]. Handbook of Chemistry and Physics, D.R. Lide ed., 73 rd ed., Sect.10, p 220, CRC press Inc., Boca Raton (USA), (1993).

[21]. PERICOLI RIDOLFINI, V., Nuclear Fusion **31**, 351 (1991), and G. Granucci, private communication (2000).

[22]. PETRZILKA,V. A., LEUTERER, F., SÖLDNER, F.X., GIANNONE, L., SCHUBERT, R., Nuclear Fusion **31**, 1757 (1991)

[23]. CRISANTI, F., LITAUDON, X., MAILLOUX, J., MAZON, D., BARBATO, E., et al. Phys. Rev, Lett., **88**, 145004, (2002).

[24]. MAILLOUX, J., ALPER, B., BARANOV, Y., BECOULET, A., CARDINALI A., et al., Phys. of Plasmas **9**, 2156 – 2164, (2002).

[25]. STANGEBY, P.C., J. Nucl. Mat. **121**, p. 55-60, (1984).

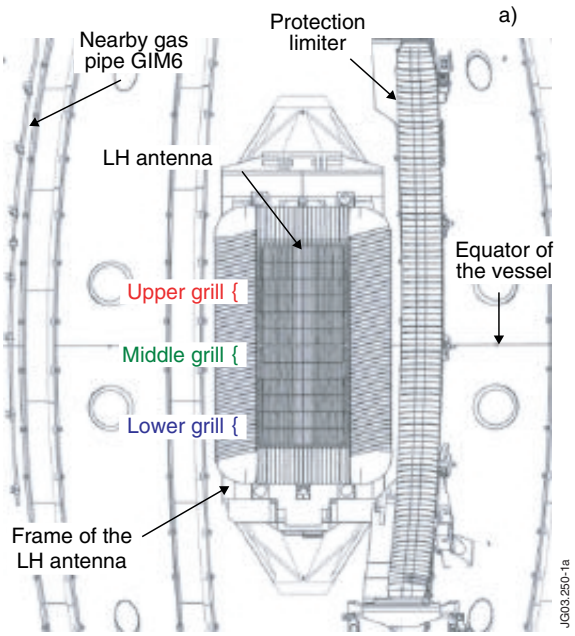

Front view of the LHCD launcher

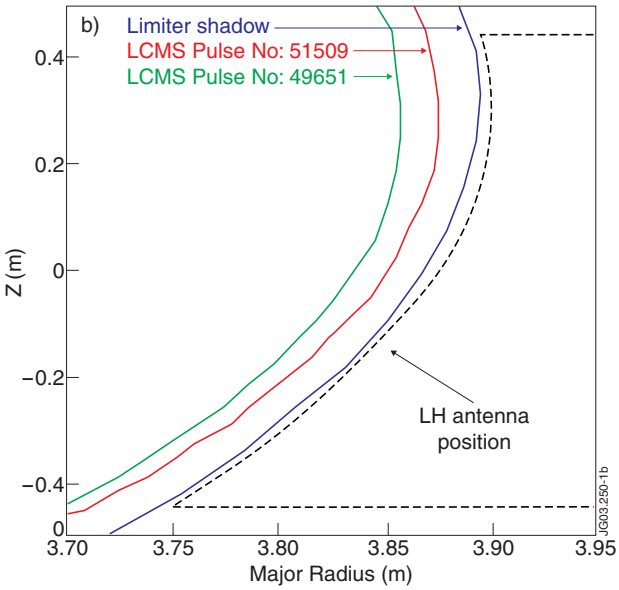

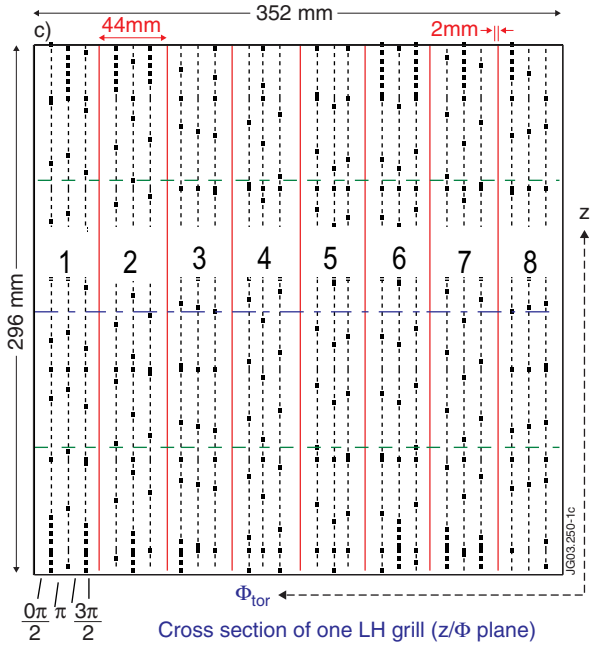

Cross section of one LH grill (z/Φ plane)

Figure 1(a) Picture of the LH launcher inserted in the JET vessel. The protection limiter and the GIM6 near gas pipe are also visible; the antenna is formed by 3 superimposed grills and is shaped along the poloidal angle as shown in b), where are also shown the profiles of the limiter and of the LCMS for an old standard ITB discharge (Pulse No: 49651) and a discharge with optimized shape; the cross section of one grill mouth perpendicularly to the propagation of the waves is sketched in c) (it is the same for the three grills). In each multijuncion, numbered from 1 to 8, there is a constant phase difference of 90^o between adjacent waveguides.

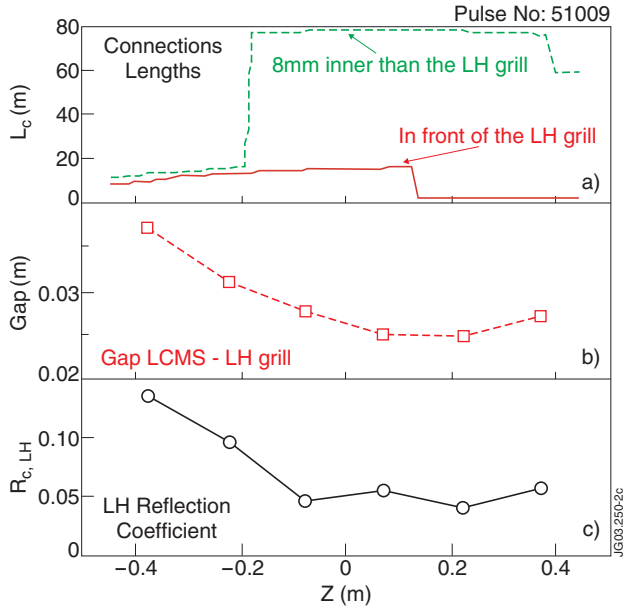

Figure 2: Poloidal pattern in front of the LH antenna of: a) The magnetic connection lengths; b) The gap between the LCMS and the LH grills; c) The LH reflection coefficient. For the frames b) and c) both the upper and the lower part of each grill are shown. A typical H-mode without optimization of the LCMS shape is shown

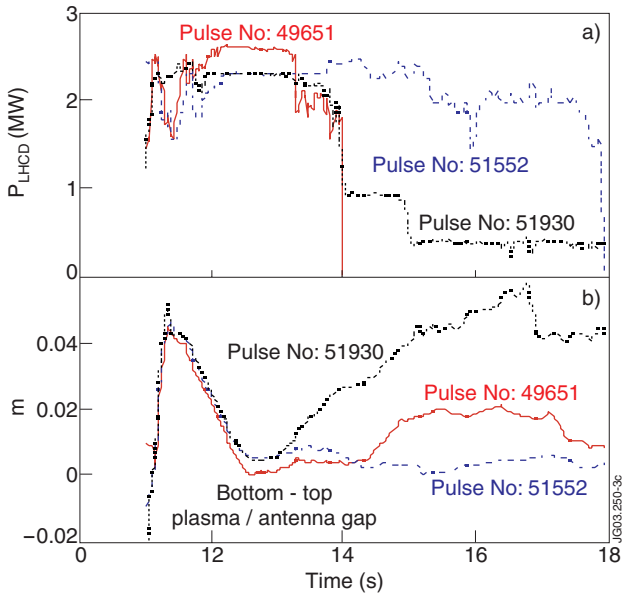

Figure 3: the result of the plasma shape optimization on the LH coupling is shown. Different shots with optimized shape (Pulse No: 51552) standard high β_p (Pulse No: 51930) and standard ITB (Pulse No: 49651) are compared: a) Coupled LH power; b) Max difference in the gap plasma-LH antenna

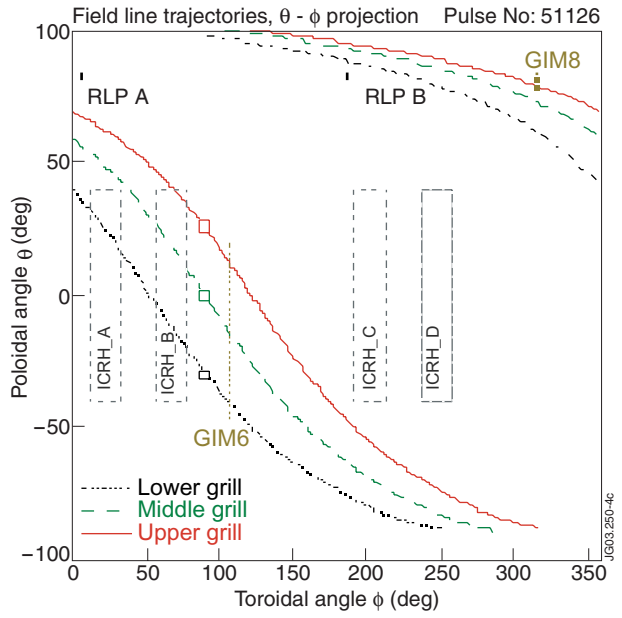

Figure 4: *Tracks of the magnetic field lines on the φ–θ plane, starting from three positions just in front of the LH grills, marked with ❐. A typical H mode or ITB plasma with I_p=2.5MA and B_T=2.6T is considered. The projections of the four ICRH antennas are shown as dashed rectangles.*

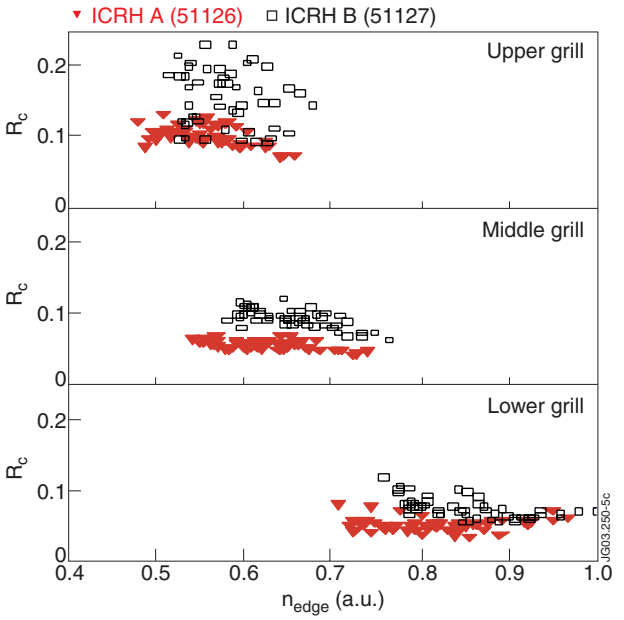

Figure 5: Behavior of the LH reflection coefficient for the three LH grills versus the normalized local edge density, which is evaluated taking into account the radial profile of the connection lengths (see text). Comparison is made between ICRH antennas B (symbol ❐, Pulse No: 51127) and A (symbol ▼, Pulse No: 51126).

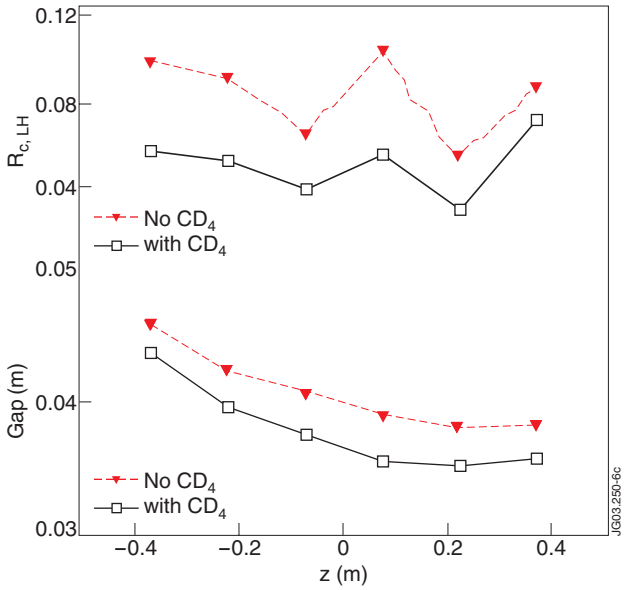

Figure 6: The effect of injecting CD_4 from the nearby gas pipe GIM6 on the LH coupling. Comparison between the cases CD_4 on/off is made for R_c in frame a), and for the LCMS-LH antenna gap in frame b). The improvement of R_c is on average larger on the worst coupled grills.

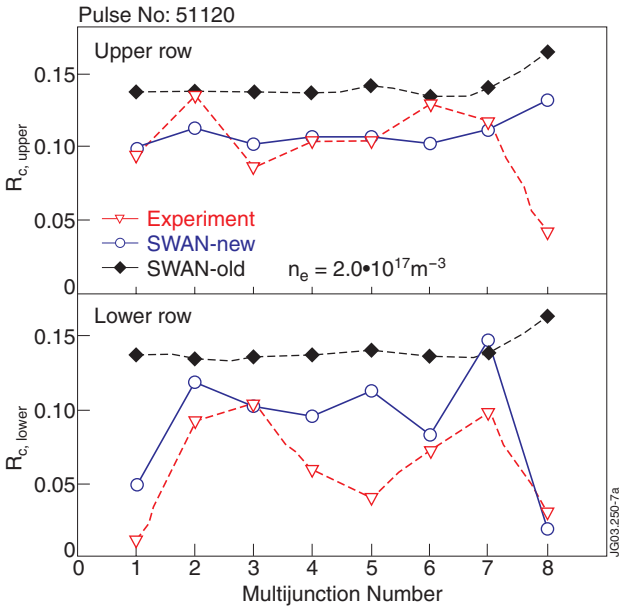

Figure 7: (a) Reflection pattern on the twomiddle rows (3 and 4) of the JET LH launcher. Dashed lines: experiment, no CD_4; solid lines: new SWAN calculations; dotted lines: old SWAN calculations. $n_{edge}= 2 \cdot 10^{17}\ m^{-3}$, d_{vac}=1mm are used in the code.

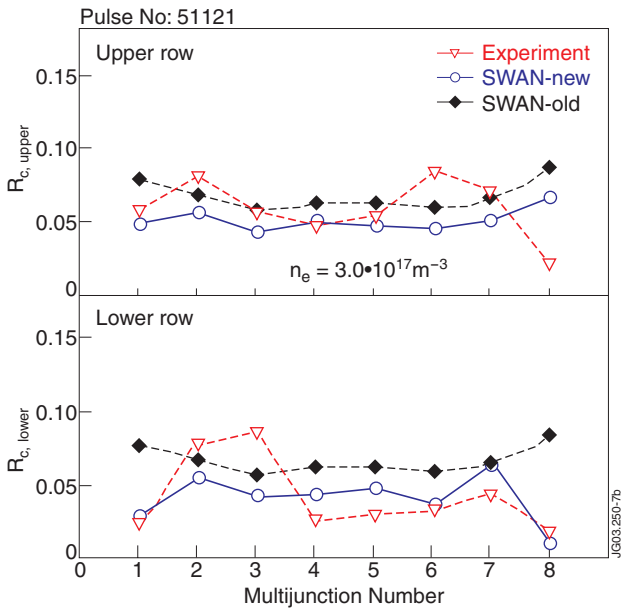

Figure 7: (b) Reflection pattern on the two middle rows (3 and 4) of the JET LH launcher. Dashed lines: experiment, CD_4 @ 10^{22} el./s; solid lines: new SWAN calculations; dotted lines: old SWAN calculations. $n_{edge}=3 \cdot 10^{17}\ m^{-3}$, d_{vac}=1mm are used in the code.

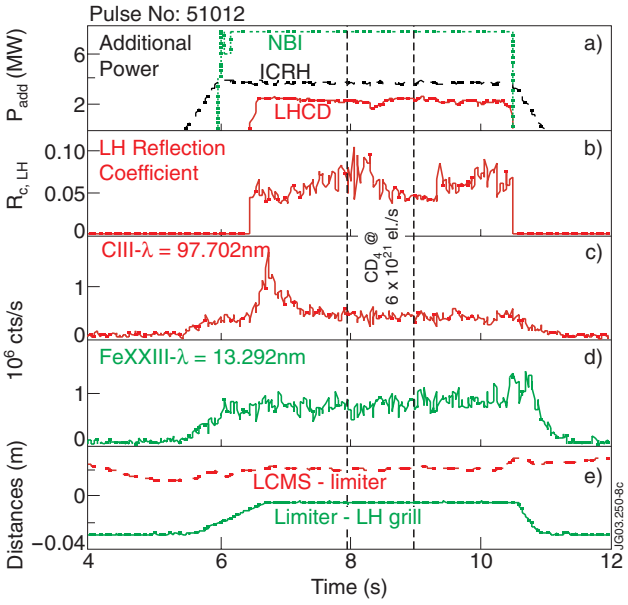

Figure 8: Effect of CD_4 puffing in an H-mode on the LH coupling and on the impurities. a) NBI, ICRH and LH powers; b) Global LH reflection coefficient; c) C III line emission @ 97.7nm, d) FeXXIII line emission @ 13.29 nm; e) position of the LH launcher, respect to the limiter, and of the central gap LCMS-LH antenna

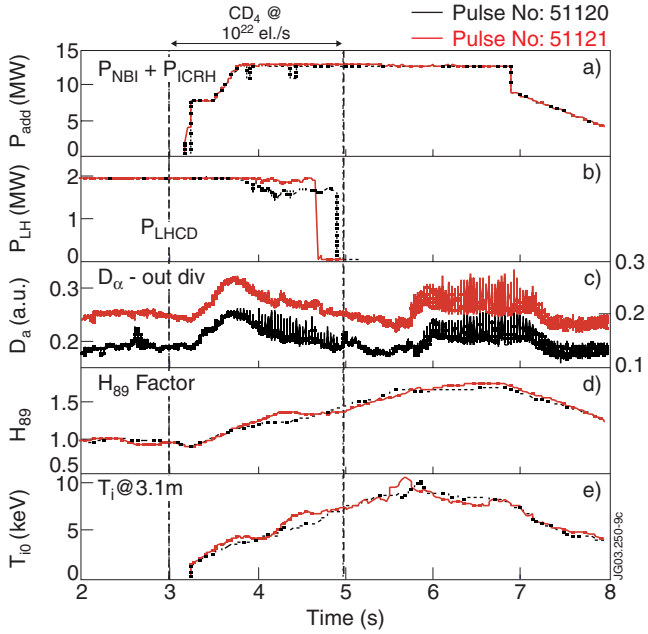

Figure 9: Effect of CD_4 puffing in ITB plasma on the development of the discharge. Two consecutive shots without/with CD_4 (Pulse No's: 51120 & 51121) are compared. a) Total ICRH+NBI power; b) LH power; c) $D\alpha$ emission from the outer divertor; d) H_{89}, enhancement confinement factor respect to ITER-89P; e) central ion temperature T_{i0}.

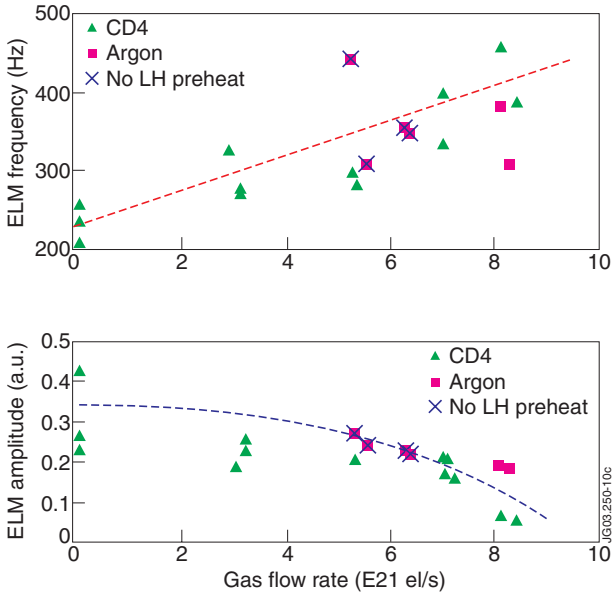

Figure 10: Effect of gas (Ar and CD_4) injection (from GIM 6) on ELM frequency and ELM magnitude for pulses with $14<P_{tot}<22$ MW. ELM frequency increases while ELM magnitude decreases when gas injection rate increases.

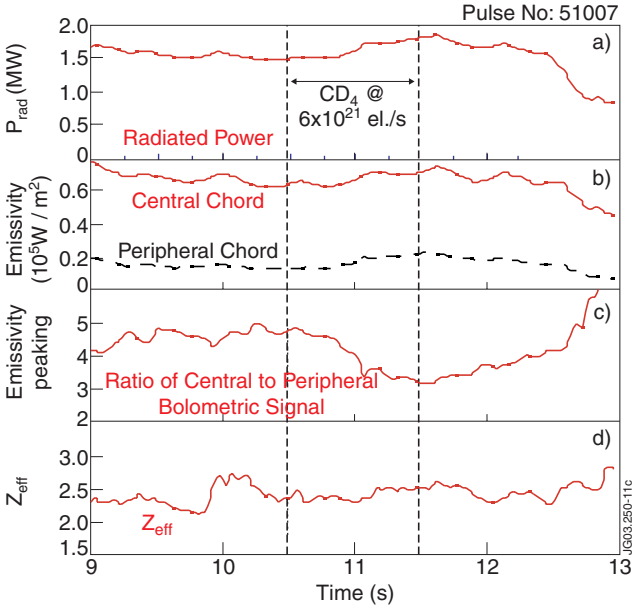

Figure 11: Variation of the radiation losses upon puffing CD_4 ($\Phi_{CD_4}=6{\cdot}10^{21}$ el./s), whose temporal gate is marked by the two dashed vertical lines. a) Total losses P_{rad}; b) line integrated value of P_{rad} along the central and a peripheral chord; c) the ratio between the previous curves; d) the average Z_{eff}.

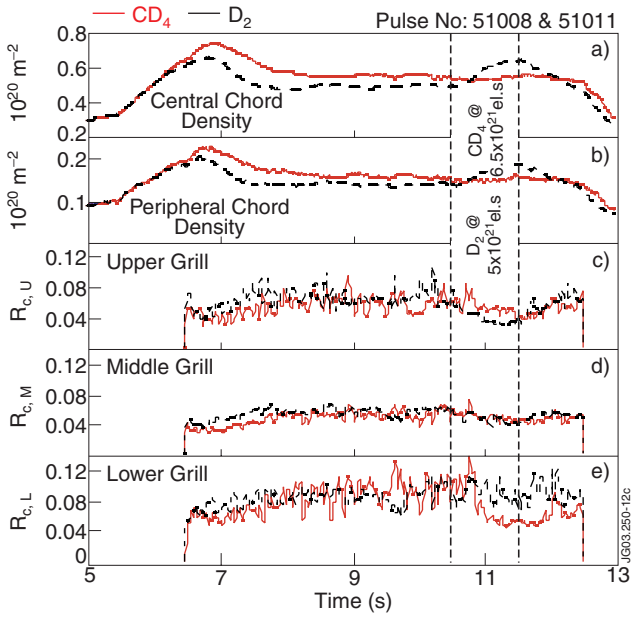

Figure 12: Comparison between CD_4 and deuterium puffing for an ELMy H-mode. The puff time window is shown with two vertical dashed lines. CD_4 and D_2 are injected from gas valves GIM6 and GIM8. Their location is shown in Fig. 4. GIM8 is not magnetically connected to the LH launcher, but it can connect if the neutral gas diffusion is considered. a), b) the line integrated value of
the density respectively on the central and on the peripheral chord of the JET interferometer; c), d), e) the LH reflection coefficient averaged respectively over the top, middle, and bottom grill. The two gas flow rates are chosen to have similar effects on R_c.

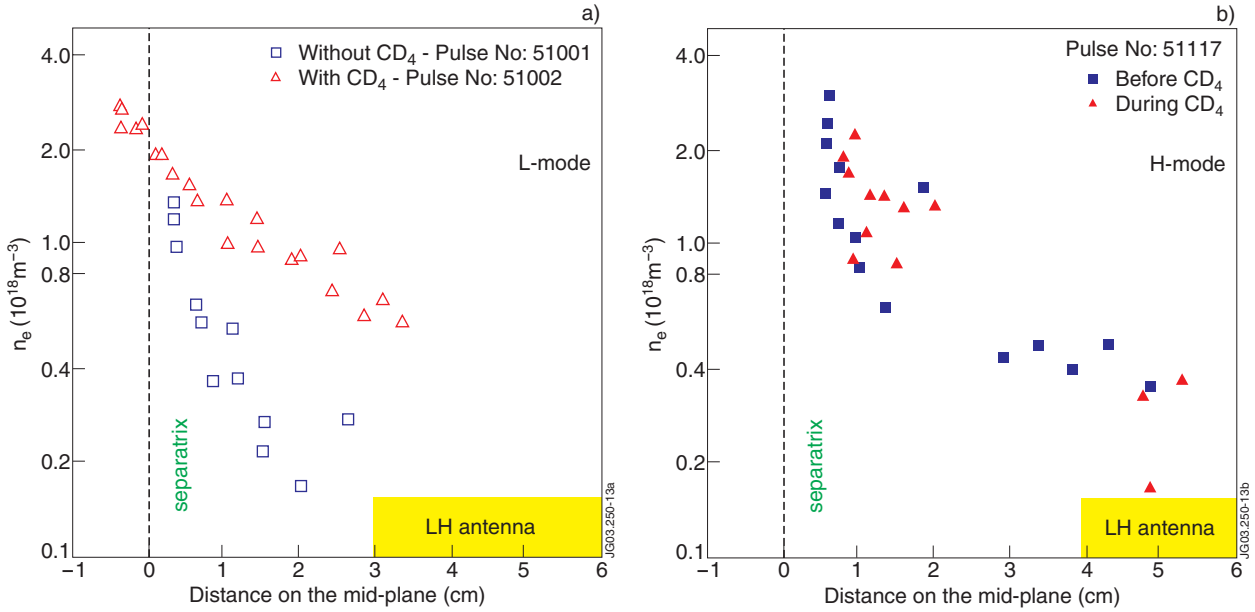

Figure 13:Radial profiles of the SOL electron density with CD_4 injection (triangles) and without (squares), according to the RLP located on the top of the octant 5 ($\varphi_{RLP}=187^o$). The abscissas are reported to the mid-plane and the position of the LH launcher is shown. In a) two identical L-mode shots are compared; in b) two radial scans at different times during a single H-mode shot are
shown, before and during CD_4 injection. For both a) and b) I_p=2.5MA and B_T=2.6T. Despite the lack of points due to disturbing effects of the ELMs on the RLP measurements, clearly no change occurs during in a H-mode.

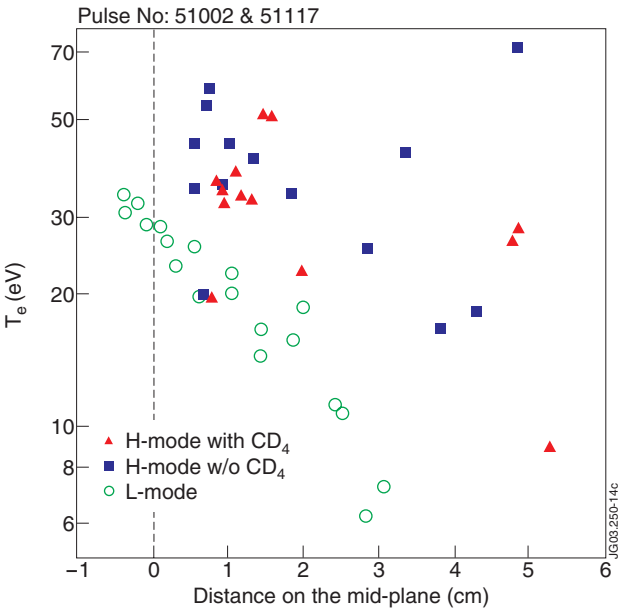

Figure 14: Plot of the radial profiles (same discharges and same RLP of the previous figure) of the SOL electron temperature in H-mode (▲ with CD_4, and ■ without) and in L-mode (❍ with CD_4). The abscissas are reported to the mid-plane. The measurements in L-mode without CD_4 are affected by a large uncertainty in the far SOL, due to the very low density and are not displayed. Despite the larger error in the H mode an average increase of T_e in the range 10-20eV is visible all along the profile.

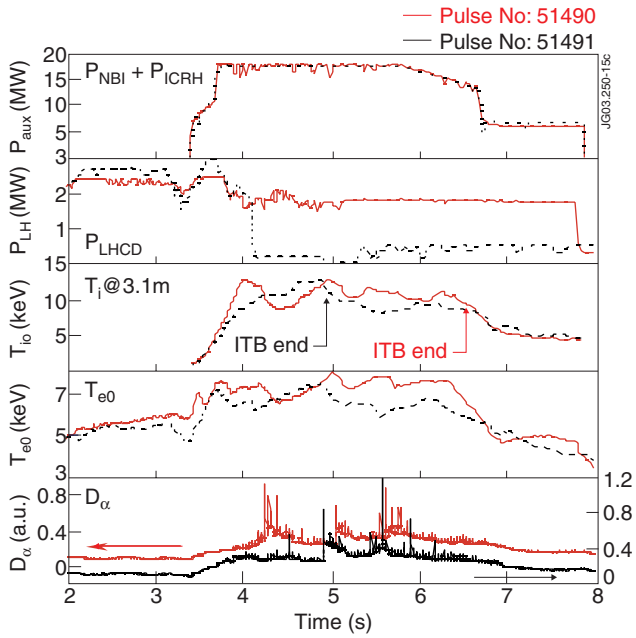

Figure 15: Most relevant time traces for ITB plasma (B_T=2.6T, I_p=2.5 MA,'n_e≈2·10^{19} m^{-3}) for two shots with LHCD during the main heating phase (Pulse No: 51490) and without LHCD (Pulse No: 51491). a) Sum of the ICRH+NBI power; b) LH power; c) Central ion temperature T_{i0}; d) Central electron temperature T_{e0}; e) D_α emission from the outer divertor plate. All the other relevant plasma quantities are the same for both shots. It is clear how the application of LH prolongs the lifetime of the ITB and helps recovering the collapses (also evidenced by the D_α signals).